Kinetic phases of distribution and tumor targeting by T cell receptor engineered lymphocytes inducing robust antitumor responses

Richard C. Koya[a,1], Stephen Mok[a], Begoña Comin-Anduix[a], Thinle Chodon[b], Caius G. Radu[c], Michael I. Nishimura[d], Owen N. Witte[c,e,f,g,1], and Antoni Ribas[a,b,g,h,1]

[a]Department of Surgery, Division of Surgical Oncology, [b]Department of Medicine, Division of Hematology/Oncology, [c]Department of Molecular and Medical Pharmacology, [e]Department of Microbiology, Immunology and Molecular Genetics, [f]Howard Hughes Medical Institute, [g]Broad Stem Cell Research Center, and [h]Jonsson Comprehensive Cancer Center, University of California, Los Angeles, CA 90095; and [d]Department of Surgery, Medical University of South Carolina, Charleston, SC 29403

Contributed by Owen N. Witte, June 18, 2010 (sent for review March 3, 2010)

A key issue in advancing the use of adoptive cell transfer (ACT) of T cell receptor (TCR) engineered lymphocytes for cancer therapy is demonstrating how TCR transgenic cells repopulate lymphopenic hosts and target tumors in an antigen-specific fashion. ACT of splenocytes from fully immunocompetent HLA-A2.1/K^b mice transduced with a chimeric murine/human TCR specific for tyrosinase, together with lymphodepletion conditioning, dendritic cell (DC)-based vaccination, and high-dose interleukin-2 (IL-2), had profound antitumor activity against large established MHC- and antigen-matched tumors. Genetic labeling with bioluminescence imaging (BLI) and positron emitting tomography (PET) reporter genes allowed visualization of the distribution and antigen-specific tumor homing of TCR transgenic T cells, with trafficking correlated with antitumor efficacy. After an initial brief stage of systemic distribution, TCR-redirected and genetically labeled T cells demonstrated an early pattern of specific distribution to antigen-matched tumors and locoregional lymph nodes, followed by a more promiscuous distribution 1 wk later with additional accumulation in antigen-mismatched tumors. This approach of TCR engineering and molecular imaging reporter gene labeling is directly translatable to humans and provides useful information on how to clinically develop this mode of therapy.

adoptive cell transfer therapy | molecular imaging | tumor immunotherapy

Adoptive cell transfer (ACT) of antigen-specific T cells involves the administration of large pools of autologous antigen-specific T cells generated by ex vivo expansion of cytotoxic T lymphocytes (CTLs) from peripheral blood mononuclear cells (PBMC) (1) or by expanding tumor antigen-reactive tumor-infiltrating lymphocytes (TIL) (2). These approaches have resulted in significant antitumor activity in patients with metastatic melanoma, but they are primarily limited by the need for lengthy ex vivo cell expansion time (several weeks) followed by the selection of antigen-specific cells for ACT. T cell receptor (TCR) engineering represents an alternative approach that attempts to shorten this process because the transfer of the alpha and beta TCR genes is necessary and sufficient to endow recipient T cells with the specificity of donor T cells (3, 4). The pioneering work by investigators at the Surgery Branch, National Cancer Institute, provided proof of principle that the ACT of TCR-engineered lymphocytes in humans is feasible and leads to objective tumor responses in patients with metastatic melanoma (5, 6).

However, early clinical studies with ACT of TCR-engineered cells suggest that their antitumor activity lags behind the response rates achieved with ACT of TILs (2). Using two different TCRs, the response rate of ACT of TCR transgenic cells to patients with metastatic melanoma was in the range of 25%, whereas the same full ACT protocol but using TILs generated response rates in the 50–70% range in patients with metastatic melanoma (6, 7). There are several possible explanations for this discrepancy, one of them being a differential trafficking of peripheral blood lymphocytes genetically modified to express transgenic TCRs compared with the ability of TILs to traffic back to peripherally located tumors. The study of the in vivo dynamics of the infused cells and how they specifically target tumors would provide information about potential problems, such as lack of specific tumor homing following ex vivo expansion, inappropriate sequestration in nonantigen positive sites, or rapid cell death and inability for the adoptively transferred TCR transgenic cells to persist in vivo. The study of these possibilities can be achieved with modern molecular imaging techniques with reporter gene labeling of cells to allow noninvasive detection of adoptively transferred TCR transgenic cell populations in recipients (8). In the current work we have taken the molecular imaging gene marking approach of antigen-specific T cells one step closer to the clinic by simultaneously redirecting the TCR specificity of T cells and providing genetic labeling for molecular imaging demonstrating robust antitumor activity correlated with specific tumor targeting.

Results

Efficient TCR and Reporter Transgene Expression and Function with 2A-Linked Viral Constructs. We used a TCR obtained from a TIL clone (TIL 1383I) that specifically recognizes the MHC class I-restricted tyrosinase$_{368–376}$ peptide presented by HLA-A2.1 (9, 10). A chimeric murine/human modification of this tyrosinase-specific TCR, with proximal constant TCR subunits being murine and the distal variable subunits being human and restricted to HLA-A2.1 (Fig. 1*A*), allowed its testing in a fully immunocompetent mouse model, recognizing tyrosinase antigen-expressing tumors that had been engineered to express a corresponding chimeric murine/human MHC molecule derived from HLA-A2.1/K^b mice (11). This modification turned the tumors syngeneic to the HLA-A2.1/K^b mice, which express the HLA-A2.1 α1 and α2 domains that allow their cells to present the same epitopes as HLA-A2.1 subjects and maintain the murine α3 domain, permitting murine CD8 coreceptor engagement (11). We generated lentiviral and retroviral vectors coexpressing the alpha and beta TCR chains of this TCR and molecular imaging reporter genes linked by picornavirus-derived "self-cleaving" 2A-like sequences (Fig. 1*B*). The 2A sequences allow the stoichiometric expression of

Author contributions: R.C.K., C.G.R., M.I.N., O.N.W., and A.R. designed research; R.C.K., S.M., B.C.-A., and T.C. performed research; R.C.K., B.C.-A., C.G.R., M.I.N., O.N.W., and A.R. contributed new reagents/analytic tools; R.C.K., C.G.R., M.I.N., O.N.W., and A.R. analyzed data; and R.C.K., O.N.W., and A.R. wrote the paper.

The authors declare no conflict of interest.

Freely available online through the PNAS open access option.

See Commentary on page 13977.

[1]To whom correspondence may be addressed. E-mail: rkoya@mednet.ucla.edu, aribas@mednet.ucla.edu or owenwitte@mednet.ucla.edu.

This article contains supporting information online at www.pnas.org/lookup/suppl/doi:10.1073/pnas.1008300107/-/DCSupplemental.

several transgenes under a single promoter in a reasonably sized gene transfer vector (12, 13), which are key features for the success of this approach. The reporter genes were luciferase for bioluminescence imaging (BLI) and an optimized herpes simplex virus 1 thymidine kinase (HSV1-tk) termed sr39tk for microPET imaging (14, 15). Transduction of cells with viral supernatants efficiently induced the expression of both alpha and beta TCR chains with more than 90% cleavage efficiency mediated by the 2A sequences as assessed by immunoblotting (Fig. 1*C*). A high level of cell surface expression of the TCRs was confirmed by flow cytometry with a clonotypic antibody to the beta chain (Fig. 1*D*) and by a specific HLA-A2.1 tetramer loaded with tyrosinase$_{368–376}$ peptide (Fig. 1*E*). The vector constructs also allowed expression of high levels of the fluorescent marker GFP (Fig. 1 *D* and *E*) concomitant with the PET reporter gene sr39tk. The functionality of sr39tk in transduced cells was analyzed by uptake of radiolabeled penciclovir (Fig. 1*F*) and by its use as a suicide gene when treated with ganciclovir (Fig. S1).

Transduced Primary T Cells Specifically Recognize Antigen-Matched Cell Targets. We then generated tyrosinase TCR retargeted primary murine T cells from HLA-A2/K^b transgenic mice by retroviral transduction with a limited expansion protocol of a total of 4 d (including the 2 d of viral vector transduction), in an attempt to limit the alteration of the functional phenotype of T cells used for ACT. These cells displayed specific functional activity demonstrated by high tyrosinase-restricted polyfunctional cytokine production (Fig. 2 and Fig. S2).

Potent Melanoma Tumor Eradication in Vivo with TCR-Transduced Syngeneic Primary T Cells. Fully immunocompetent HLA-A2/K^b transgenic mice with flank B16-A2/K^b murine melanoma tumors of 4 mm average diameters underwent whole body myelodepleting irradiation followed by i.v. ACT of tyrosinase TCR-transduced syngeneic splenocytes, tyrosinase$_{368–376}$ peptide-pulsed DC vaccination, and high-dose IL-2 (Fig. 3*A*). The melanoma tumors grew rapidly in the control group where mice received the complete therapy including myelodepletion, DC vaccination, and IL-2 but the splenocytes were transduced with a control retrovirus. Mice receiving adoptive transfer of tyrosinase TCR T cells had robust antitumor activity (Fig. 3*B*) and improved survival (P = 0.0006).

In Vivo T Cell Tracking with Bioluminescence Imaging Shows Discrete Patterns of TCR Transgenic Distribution and Specific Tumor Targeting. ACT of TCR transgenic cells need to repopulate a lymphopenic host, expand in vivo, target antigen-matched tumors, and then exert their specific cytotoxic activity. This process can be sequentially studied using noninvasive molecular imaging. HLA-A2/K^b transgenic mice had isogenic tumors implanted that stably expressed tyrosinase (EL4-A2/K^b-Tyr) or did not express this tumor antigen (EL4-A2/K^b) in contralateral lower abdominal flanks. When tumors reached average diameters of 6 mm, mice were conditioned with whole body irradiation and then received i.v. ACT of tyrosinase TCR/firefly luciferase retroviral vector-transduced syngeneic T cells, tyrosinase$_{368–376}$ peptide

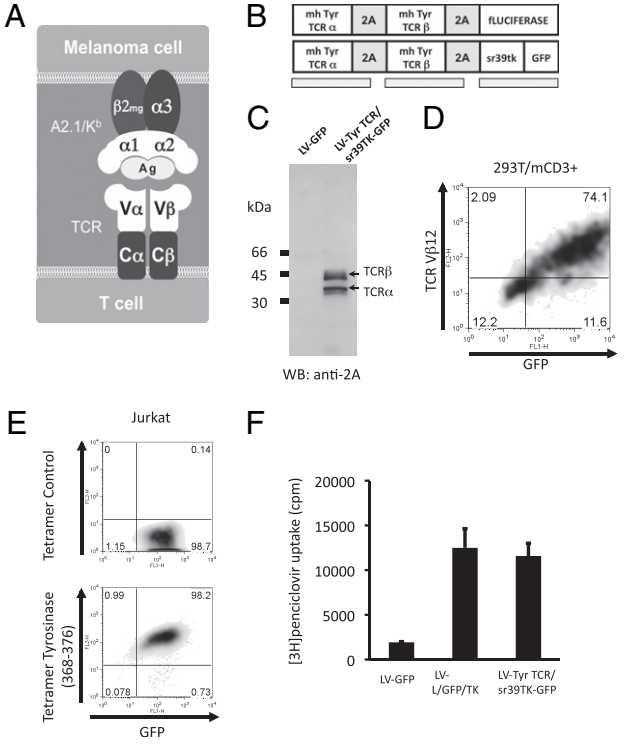

Fig. 1. Model system, vector schematic, and transgene expression. (*A*) Schematic of the chimeric murine/human interaction between the transgenic TCR and MHC molecules in the A2.1/K^b mouse model. In gray are the proximal murine sequences, and in white the distal human sequences allowing the presentation and recognition of peptide antigen with human restriction. (*B*) Tyrosinase (Tyr)-TCR/sr39TK-GFP and firefly luciferase vector schematic representation. (*C*) Immunoblotting of 293T cells transduced with control lentiviral vector expressing GFP (LV-GFP) or the tyrosinase TCR and sr39tk (LV-TCR/sr39TK-GFP) vectors, incubation with rabbit anti-2A primary antibody. Arrows indicate cleaved products with sizes corresponding to the TCR α and β chains. (*D*) Flow-cytometric analysis of 293T cells expressing CD3 transduced with LV-TCR/sr39TK-GFP vector, stained with specific clonotypic anti-Vβ12 antibody. (*E*) Tyrosinase$_{368–376}$ specific and negative control peptide HLA-A2.1 tetramer assay of Jurkat cells transduced with LV-TCR/sr39TK-GFP vector. (*F*) Penciclovir uptake assay of Jurkat cells transduced with negative control LV-GFP, positive control LV-L/GFP/TK, or LV-TCR/sr39TK-GFP vectors.

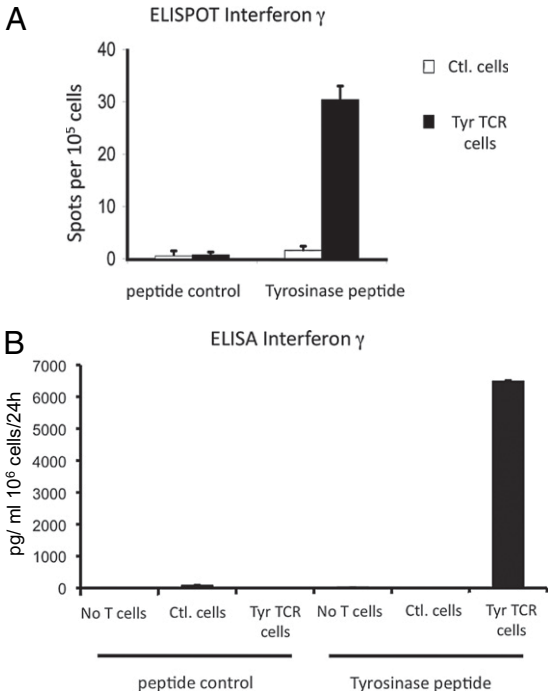

Fig. 2. In vitro functional analysis of murine primary T cells transduced with tyrosinase TCR retroviral supernatants. (*A*) ELISPOT assay for cellular IFN-γ secretion of control T cells and tyrosinase TCR transduced T cells incubated with control scrambled or tyrosinase$_{368–376}$ peptides. (*B*) ELISA for total IFN-γ secretion of 24 h-collection supernatants of EL4-A2/K^b pulsed with control or tyrosinase peptides coincubated with control T cells or tyrosinase TCR transduced T cells.

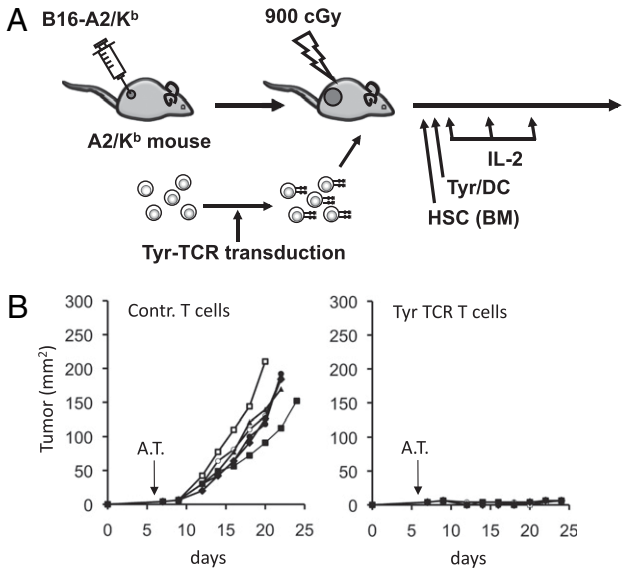

Fig. 3. In vivo function of murine primary T cells transduced with tyrosinase TCR retrovirus. (*A*) HLA-A2/K^b transgenic mice with s.c. B16-A2/K^b tumors received the full protocol of myelodepletion with hematopoietic stem cells (HSC)/ bone marrow (BM) transplantation, adoptive cell transfer (ACT) of control T cells or tyrosinase TCR-transduced T cells followed by tyrosinase$_{368–376}$ peptide-pulsed dendritic cell (DC) vaccination and high-dose IL-2. (*B*) Mice were followed for tumor growth measurements (product of two diameters as mm^2), $P < 0.01$.

pulsed DCs, and high-dose IL-2 with serial BLI of T cell localization and persistence. After an initial brief period of systemic distribution, a strong BLI signal was observed in the tyrosinase-expressing tumors with peak intensity on day 5 after ACT (Fig. 4*A* and Fig. S3). The decrease in BLI intensity paralleled the corresponding marked tumor shrinkage in response to tyrosinase TCR ACT therapy (Fig. 4*B*). The BLI signal on tyrosinase negative tumors was relatively low initially, but gradually increased as the tumors grew in size (Fig. 4*A*). We confirmed the identity of adoptively transferred tyrosinase TCR/firefly luciferase T cell accumulation in the tumors and lymph nodes by CD4, CD8, and luciferase immunofluorescence staining of histological sections (Fig. 4*C*).

Micro-PET/CT Imaging of TCR-Transduced T Cell Localization with Higher Spatial Refinement and Quantification Confirming the Phases of T Cell Distribution in Vivo. There is signal attenuation from deep tissues with BLI analysis, which may limit the study of tyrosinase TCR transgenic cell distribution in vivo and its clinical applicability. Therefore, to confirm the findings with an approach with higher spatial/anatomical localization of ACT with engineered tyrosinase TCR T cells, micro-PET/CT imaging was used. Murine T cells were transduced with a retroviral vector coexpressing tyrosinase TCR and sr39tk-GFP and adoptively transferred i.v. to syngeneic mice with EL4-A2/K^b tumors expressing tyrosinase and negative control EL4-A2/K^b tumors (Fig. S4) or B16-A2/K^b murine melanoma tumors (Fig. 5) and followed over different time periods. The phases of tyrosinase TCR transgenic cell distribution upon ACT defined by BLI were confirmed with PET imaging. As observed in the BLI studies, tyrosinase TCR transgenic T cells equally distributed to both tyrosinase positive and negative tumors on day 1. Scans on subsequent days showed higher accumulation of tyrosinase TCR T cells in tyrosinase-expressing tumors (Fig. S4) followed by a final phase of systemic distribution. With the higher spatial resolution provided by micro-PET/CT imaging, a punctuated pattern demonstrating a heterogeneous accumulation of T cells within the tumor confinements could be observed (Fig. 5*A* and Fig. S4). Another advantage of micro-PET/CT imaging is the possibility of tridimensional imaging reconstruction (Fig. 5*B* and Movie S1). Because [^{18}F]FHBG tracer scans in mice (but not in humans) (16) have high nonspecific background signal in organs involved in its clearance such as bladder, kidneys, ureters, liver, gall bladder, and intestines, the signals from these organs were subtracted (Fig. S4). The utilization of Fenestra VC contrast agent for CT imaging allowed us to analyze and quantify the signal localized in the spleen (Fig. 5*B* and Fig. S4*B*). In addition, micro-PET/CT scanning could distinguish discrete signal corresponding to axillary lymph nodes from the closely located tumor (Fig. 5*B*).

Discussion

This work demonstrates a close relationship between antitumor activity and early specific antigen homing of TCR-engineered ACT therapy. This was achieved using lymphocytes that were simultaneously genetically redirected and labeled to allow the generation of large numbers of uniformly antigen-specific cells that could be visualized as they accumulated in tumors expressing their cognate antigen, leading to profound antitumor activity using this system. We demonstrate that the i.v. adoptive transfer of tyrosinase TCR-engineered T cells to lymphopenic hosts goes through an orderly systemic distribution and antigen-specific tumor targeting.

There is a need to optimize the ACT of TCR transgenic cells to achieve the antitumor activity levels of ACT with TIL (2). Improvements in viral vector design, high-efficiency gene modification of lymphocytes, and selection of TCR chains with dominant pairing or with molecular alterations to avoid mispairing with endogenous TCR chains (6, 17) allow rapid generation of large pools of antigen-specific lymphocytes for ACT with limited ex vivo manipulation. The limitation derived from the need for ex vivo expansion of lymphocytes to transduce T cells is important because this process is likely to modify the phenotype and function of these cells (18), resulting in altered in vivo distribution to secondary lymphoid organs and peripheral tissues. Potential scenarios include the inability of T cells to maintain a naïve phenotype with this manipulation, the loss of specific memory T cell phenotypes, and the acquisition of late effector or exhausted T cell phenotypes with prolonged ex vivo expansion (19). Therefore, minimizing ex vivo manipulation and analyzing the in vivo kinetics of adoptively transferred cells would allow optimization of this therapeutic approach.

Our fully immunocompetent and syngeneic animal model should be useful for the testing of the distribution of TCR transgenic cells with relevance to the clinic. It provides a significant advancement over xenogeneic ACT studies in immunodeficient animals (20), because those studies lack fully developed lymphoid organs and therefore cannot provide deeper insight into the engraftment and biodistribution of adoptively transferred TCR-engineered T cells. In a clinical scenario, the patient's own peripheral blood T cells would be engineered to express TCR specific to tumor antigens, which is similar to our use of murine splenocytes with limited ex vivo manipulation to insert TCR genes and molecular imaging genes. Using this model we demonstrated that the retargeted T cells are very efficient in controlling specific tumor growth in vivo and they localized in different organs in an exquisite temporal pattern. The model could be expanded to preclinically screen the in vivo function of newly cloned TCRs, because HLA-A2.1 is the most prevalent HLA allele in the general population, accounting for roughly 45% of patients with metastatic melanoma. Consequently, HLA-A2/K^b transgenic mice provide a powerful model to study human MHC class I-restricted antigen epitopes recognized by human T cells, which potentially provide a direct application of the same TCRs studied in these transgenic mice for future clinical use.

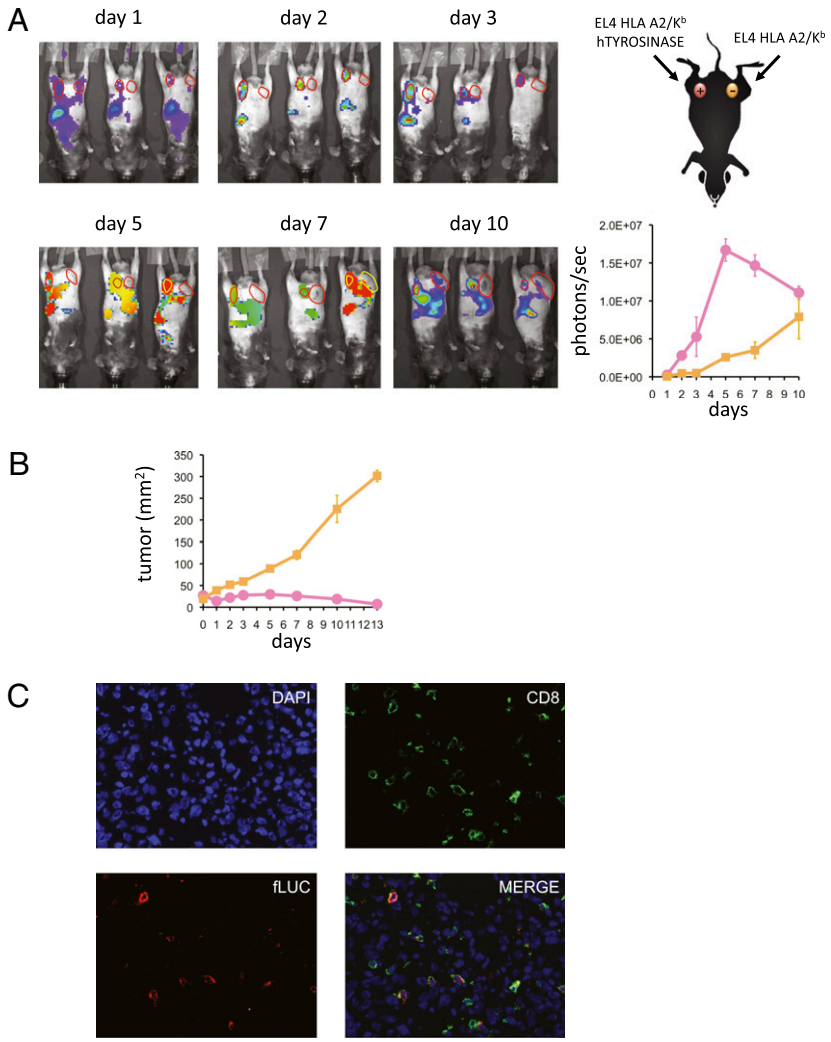

Fig. 4. Bioluminescence imaging (BLI) of T cell trafficking in vivo. (*A*) HLA-A2/K^b transgenic mice with inguinal s.c. EL4-A2/K^b-expressing tyrosinase (*Left*) and control EL4-A2/K^b (*Right*) tumors received the full protocol of adoptive cell transfer (ACT) with tyrosinase TCR/fLuciferase-transduced T cells. Mice were followed from day 1 to 10 post-ACT and bioluminescence signal of ventral views were recorded and quantified on region of interest (ROI) drawn on tumor sites. Representative animals are shown. Pink, EL4-A2/K^b-tyrosinase+; yellow, control EL4-A2/K^b. (*B*) These mice were followed for tumor growth measurements (product of two diameters as mm^2). (*C*) EL4-A2/K^b-tyrosinase+ tumors were costained with DAPI (nucleus localization), anti-CD8, and anti-fLuciferase (40×).

The definition of the pattern of distribution of adoptively transferred cells eliciting robust antitumor activity can be used to later analyze individual components of this combinatorial approach before going into clinical trials. In addition to screening different TCRs with human MHC class I restriction elements, variables like the surface functional phenotype of lymphocytes and their skewing while being activated ex vivo for TCR transduction affecting their in vivo distribution upon ACT, the maximization of cell persistence in vivo and the role of supporting therapies like the conditioning regimen, the use of high-dose IL-2, and antigen-specific vaccines can be systematically analyzed. Therefore, molecular imaging with reporter genes enables monitoring of adoptively transferred TCR-engineered retargeted cells to study their biodistribution, expansion/contraction, and persistence, allowing pattern-based prediction of T cell-based immunotherapeutic efficiency and clinical outcome.

Materials and Methods

Subcloning and Vector Construction. The α and β chains of the TIL 1383I TCR (9, 10) had their corresponding constant regions entirely substituted with murine counterparts by standard PCR techniques to generate a hybrid human/murine TCR construct. The 2A self-cleaving sequences were inserted between the transgenes by overlap PCR (12, 13). The whole construct was then inserted into a self-inactivating third generation lentiviral vector (21) or a retroviral vector derived from a murine stem cell virus (pMSCV) backbone (22) containing a 5′ long terminal repeat-driven truncated version of the sr39tk (15) fused with enhanced green fluorescent protein (eGFP), or a firefly luciferase gene (14). To obtain the HLA-A2/K^b transgene to engineer syngeneic tumor targets, total mRNA was obtained from hepatocytes of HLA-A2/K^b transgenic mice (from Linda Sherman, The Scripps Research Institute, La Jolla, California) (11). This HLA-A2/K^b transgene was inserted into a lentiviral vector with a MND-driven promoter (23) and used to transduce B16 and EL4 cells to generate the cell lines B16-A2/K^b and EL4-A2/K^b, respectively. Similarly, the full-length human tyrosinase cDNA was obtained by PCR cloning and used to generate a lentiviral vector with MND promoter for the transduction of EL4-A2/K^b cells to express the tyrosinase gene (EL4-A2/K^b-Tyr).

Analysis of Transgene Expression by TCR Engineering Viral Vectors. Lentivirus vectors were produced using a transient transfection protocol (21). Testing of transgene expression was performed by transducing 293T-CD3 cells (from David Baltimore, California Institute of Technology, Pasadena, California). Cells were analyzed by Western blot using an anti-2A antibody (from Dario Vignali, St. Jude Children's Research Hospital, Memphis, Tennessee) as previously described (13). TCR expression upon transduction of 293T-CD3, the

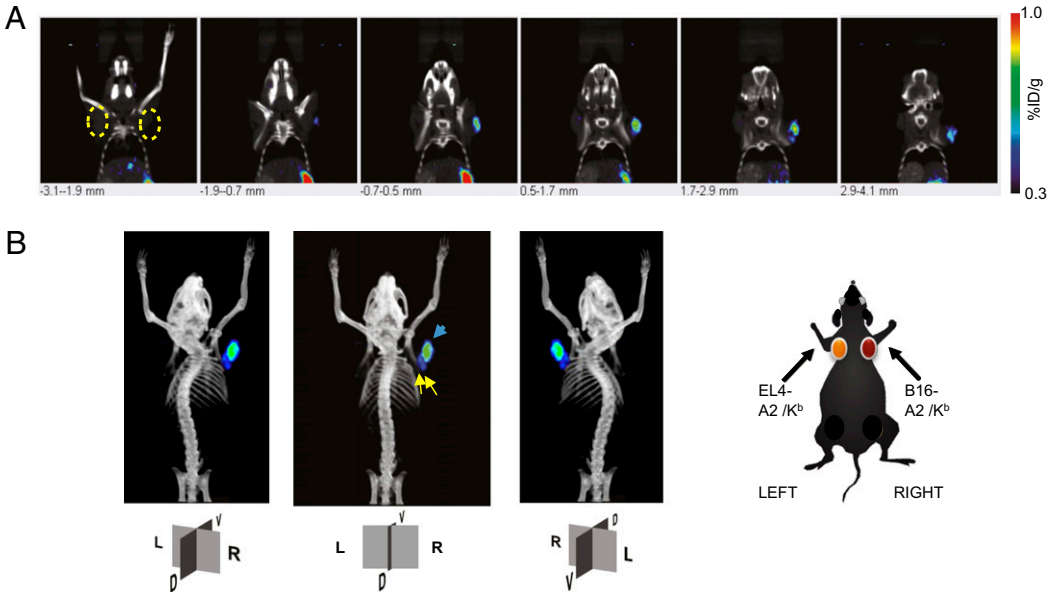

Fig. 5. PET CT imaging of T cell trafficking in vivo in mice with control EL4-A2/K^b tumors or with contralateral tyrosinase-positive B16-A2/K^b tumors at day 5 post-ACT. (*A*) HLA-A2/K^b transgenic mice with thoracic dorsal s.c. B16-A2/K^b (*Right*) and control EL4-A2/K^b (*Left*) tumors were adoptively transferred with tyrosinase TCR/sr39TK/GFP transduced T cells. Representative animals are shown. Specific signal quantification ratio above background: *Left* ROI = 1.05 ± 0.59%ID/g; *Right* ROI = 3.00 ± 0.61%ID/g. (*B*) Schematic representation of tumor location and reconstructed tridimensional PET CT scan image with the nonspecific signal from abdominal excretion of [^{18}F]FHBG subtracted from the final image. Yellow arrows, signals on axillary lymph nodes (specific signal quantification ratio above background: *Right* LND = 2.21 ± 0.52%ID/g; *Left* LND = 2.05 ± 0.63%ID/g). Blue arrow, signal in B16-A2/K^b tumor. R, right; L, left; D, dorsal; V, ventral sides.

human T cell lymphoma line Jurkat or primary murine splenocytes was analyzed by flow cytometry using a clonotypic TCR β12 antibody (BD Biosciences) and tyrosinase$_{368–376}$ MHC tetramers (Beckman Coulter). An in vitro ganciclovir lysis assay was performed by adding titrated amounts of ganciclovir to transduced 293T-CD3 cells and viable cells analyzed by an MTS assay. For ^{3}H-Penciclovir accumulation assays, transduced and control untransduced cells incubated for 120 min with [^{3}H]-Penciclovir at 3.7 kBq/mL (1.48 TBq/mmol) (Moravek Biochemicals) were assayed for radioactivity concentrations with a TriCarb 1600 β-spectrometer (Canberra Packard).

In Vitro Activation of Murine T Cells and Viral Vector Transduction. High-titer helper-free lentivirus or retrovirus stocks were prepared by transient cotransfection of 293T cells (21). RBC lysed murine splenocytes from HLA-A2/K^b transgenic mice were cultured in X-Vivo 15 (Biowhittaker) supplemented with 10% heat inactivated FBS (HyClone), 50 μM β-mercapto-ethanol and 50 IU/mL of rhIL-2 (Novartis) with anti-CD3 and anti-CD28-coated plates (BD Biosciences). At 48 h postactivation, cells underwent two rounds of spinfection with retrovirus supernatants (10 multiplicity of infection) in retronectin (Takara Bio) coated plates at 1,000 g, 120 min, 32 °C.

Adoptive Transfer, Vaccination, and Tumor Treatment. HLA-A2/K^b transgenic mice had s.c. B16-A2/K^b tumor implanted, or EL4-A2/K^b tumors expressing or not expressing tyrosinase protein. When tumors reached 4–6 mm in diameter, lymphopenia was induced by sublethal irradiation (500 cGy) or myeloablation with 900 cGy irradiation (followed by bone marrow transplant as described in ref. 24). On the next day (day 0), groups of mice were randomized into control marker vector or tyrosinase TCR vector transduced cells for i.v. (tail vein) injection. DCs were differentiated from bone marrow progenitor cells obtained from HLA-A2/K^b mice by in vitro culture in murine granulocyte macrophage colony-stimulating factor (GM-CSF, 50 ng/mL) and murine IL-4 (50 ng/mL; R&D Systems) as described (25) and pulsed with tyrosinase$_{368–376}$ peptide at 10 μM in serum-free media for 90 min at room temperature. Each mouse received 10^5 pulsed DCs s.c. on day 0. Recombinant human IL-2 (250,000 IU) was injected intraperitoneally on days 0, 1, and 2. Murine studies were performed under the University of California Los Angeles Animal Research Committee (ARC) approval number 2004–159.

Functional Antigen Recognition Assays. Transduced cells were tested for tyrosinase-specific reactivity by coculturing responder cells with stimulator cells in a 1:1 ratio in 96-well U-bottomed plates. Stimulator cells included tyrosinase$_{368–376}$ peptide-pulsed or unpulsed K562-A2.1, EL4-A2/K^b, EL4-A2/K^b-Tyr, or B16-A2/K^b cells. The amount of IFN-γ released was measured by ELISA (R&D Systems) and ELISPOT assays as described (26). For the multiplex cytokine-release assay, supernatants were obtained at 24, 48, and 72 h of coincubation and analyzed following the manufacturer's instructions using a Bio-Plex Mouse Cytokine Panel (Bio-Rad Laboratories).

Bioluminescence Imaging (BLI). BLI was performed with a Xenogen IVIS 200 Imaging System (Xenogen/Caliper Life Sciences) as previously described (14).

Micro-PET/Computed Tomography Imaging. Mice were anesthetized with 2% isoflurane. PET was performed 1 h after i.v. administration of 7.4 MBq (200 μCi) of [^{18}F]FHBG and mice were scanned using a FOCUS 220 micro-PET scanner (Siemens) (energy window of 350–750 keV and timing window of 6 ns) as described previously (15). Additional details on the performance of PET scans are included in *SI Materials and Methods*.

Histological Analysis. Freshly isolated tissues were frozen in optimum cutting temperature (OCT) compound (Sakura Finetek). The immunohistochemical reaction was carried out with the following antibodies: rat anti-mCD4 or anti-mCD8 (BD Biosciences), and rabbit anti-fLuciferase (Abcam) and then with secondary donkey anti-rat antibodies conjugated to DyLight 488 and anti-rabbit DyLight 549 (Jackson Immunoresearch Laboratories), respectively, with 4,6-diamidino-2-phenylindole for nuclei visualization. Immunofluorescence was assessed with a fluorescence microscope (Carl Zeiss).

Statistical Analysis. Data were analyzed with GraphPad Prism (version 5) software (GraphPad Software). A Mann–Whitney test or ANOVA with Bonferroni posttest was used. Survival analysis was performed with the Kaplan–Meier method, and curves were compared in a log-rank test.

ACKNOWLEDGMENTS. This work was funded by the National Institutes of Health Award P50 CA086306, the California Institute for Regenerative Medicine New Faculty Award RN2-00902-1, the California Institute of Technology–University of California Los Angeles Joint Center for Translational Medicine (to A.R.), and the California Institute for Regenerative Medicine Tools and Technology Award RT1-01126 (to C.G.R.). R.C.K. was supported by the V Foundation-Gil Nickel Family Endowed Fellowship in Melanoma Research. O.N.W. is an investigator of the Howard Hughes Medical Institute.

1. Yee C, et al. (2002) Adoptive T cell therapy using antigen-specific CD8+ T cell clones for the treatment of patients with metastatic melanoma: In vivo persistence, migration, and antitumor effect of transferred T cells. *Proc Natl Acad Sci USA* 99:16168–16173.
2. Rosenberg SA, Restifo NP, Yang JC, Morgan RA, Dudley ME (2008) Adoptive cell transfer: A clinical path to effective cancer immunotherapy. *Nat Rev Cancer* 8:299–308.
3. Dembić Z, et al. (1987) Transfection of the CD8 gene enhances T-cell recognition. *Nature* 326:510–511.
4. Schumacher TN (2002) T-cell-receptor gene therapy. *Nat Rev Immunol* 2:512–519.
5. Morgan RA, et al. (2006) Cancer regression in patients after transfer of genetically engineered lymphocytes. *Science* 314:126–129.
6. Johnson LA, et al. (2009) Gene therapy with human and mouse T-cell receptors mediates cancer regression and targets normal tissues expressing cognate antigen. *Blood* 114:535–546.
7. Dudley ME, et al. (2008) Adoptive cell therapy for patients with metastatic melanoma: Wvaluation of intensive myeloablative chemoradiation preparative regimens. *J Clin Oncol* 26:5233–5239.
8. Dubey P, et al. (2003) Quantitative imaging of the T cell antitumor response by positron-emission tomography. *Proc Natl Acad Sci USA* 100:1232–1237.
9. Nishimura MI, et al. (1999) MHC class I-restricted recognition of a melanoma antigen by a human CD4+ tumor infiltrating lymphocyte. *Cancer Res* 59:6230–6238.
10. Roszkowski JJ, et al. (2003) CD8-independent tumor cell recognition is a property of the T cell receptor and not the T cell. *J Immunol* 170:2582–2589.
11. Vitiello A, Marchesini D, Furze J, Sherman LA, Chesnut RW (1991) Analysis of the HLA-restricted influenza-specific cytotoxic T lymphocyte response in transgenic mice carrying a chimeric human-mouse class I major histocompatibility complex. *J Exp Med* 173:1007–1015.
12. de Felipe P, Martín V, Cortés ML, Ryan M, Izquierdo M (1999) Use of the 2A sequence from foot-and-mouth disease virus in the generation of retroviral vectors for gene therapy. *Gene Ther* 6:198–208.
13. Szymczak AL, et al. (2004) Correction of multi-gene deficiency in vivo using a single 'self-cleaving' 2A peptide-based retroviral vector. *Nat Biotechnol* 22:589–594.
14. Prins RM, et al. (2008) Anti-tumor activity and trafficking of self, tumor-specific T cells against tumors located in the brain. *Cancer Immunol Immunother* 57:1279–1289.
15. Shu CJ, et al. (2009) Quantitative PET reporter gene imaging of CD8+ T cells specific for a melanoma-expressed self-antigen. *Int Immunol* 21:155–165.
16. Yaghoubi SS, et al. (2005) Imaging progress of herpes simplex virus type 1 thymidine kinase suicide gene therapy in living subjects with positron emission tomography. *Cancer Gene Ther* 12:329–339.
17. Kuball J, et al. (2007) Facilitating matched pairing and expression of TCR chains introduced into human T cells. *Blood* 109:2331–2338.
18. Hinrichs CS, et al. (2009) Adoptively transferred effector cells derived from naive rather than central memory CD8+ T cells mediate superior antitumor immunity. *Proc Natl Acad Sci USA* 106:17469–17474.
19. Klebanoff CA, Gattinoni L, Restifo NP (2006) CD8+ T-cell memory in tumor immunology and immunotherapy. *Immunol Rev* 211:214–224.
20. Bobisse S, et al. (2009) Reprogramming T lymphocytes for melanoma adoptive immunotherapy by T-cell receptor gene transfer with lentiviral vectors. *Cancer Res* 69: 9385–9394.
21. Koya RC, Kasahara N, Pullarkat V, Levine AM, Stripecke R (2002) Transduction of acute myeloid leukemia cells with third generation self-inactivating lentiviral vectors expressing CD80 and GM-CSF: Effects on proliferation, differentiation, and stimulation of allogeneic and autologous anti-leukemia immune responses. *Leukemia* 16: 1645–1654.
22. Hawley RG, Lieu FH, Fong AZ, Hawley TS (1994) Versatile retroviral vectors for potential use in gene therapy. *Gene Ther* 1:136–138.
23. Robbins PB, et al. (1997) Increased probability of expression from modified retroviral vectors in embryonal stem cells and embryonal carcinoma cells. *J Virol* 71:9466–9474.
24. Wrzesinski C, et al. (2007) Hematopoietic stem cells promote the expansion and function of adoptively transferred antitumor CD8 T cells. *J Clin Invest* 117:492–501.
25. Ribas A, et al. (1997) Genetic immunization for the melanoma antigen MART-1/ Melan-A using recombinant adenovirus-transduced murine dendritic cells. *Cancer Res* 57:2865–2869.
26. Comin-Anduix B, et al. (2008) Detailed analysis of immunologic effects of the cytotoxic T lymphocyte-associated antigen 4-blocking monoclonal antibody tremelimumab in peripheral blood of patients with melanoma. *J Transl Med* 6:22.